Algorithmic methods to infer the evolutionary trajectories in cancer progression

Giulio Caravagna[a,b,1], Alex Graudenzi[a,c], Daniele Ramazzotti[a], Rebeca Sanz-Pamplona[d,e,f], Luca De Sano[a], Giancarlo Mauri[a,g], Victor Moreno[d,e,f,h], Marco Antoniotti[a,i], and Bud Mishra[j]

[a]Department of Informatics, Systems and Communication, University of Milan-Bicocca, 20126 Milan, Italy; [b]School of Informatics, University of Edinburgh, Edinburgh EH8 9YL, United Kingdom; [c]Institute of Molecular Bioimaging and Physiology, Italian National Research Council, 93-I-20090 Milan, Italy; [d]Unit of Biomarkers and Susceptibility, Cancer Prevention and Control Program, Catalan Institute of Oncology, Hospitalet de Llobregat, 08908 Barcelona, Spain; [e]Bellvitge Institute for Biomedical Research, Hospitalet de Llobregat, 08908 Barcelona, Spain; [f]Biomedical Research Centre Network for Epidemiology and Public Health, Hospitalet de Llobregat, 08908 Barcelona, Spain; [g]SYSBIO Centre of Systems Biology (SYSBIO), 20126 Milan, Italy; [h]Department of Clinical Sciences, Faculty of Medicine, University of Barcelona, 08007 Barcelona, Spain; [i]Milan Center for Neuroscience, University of Milan-Bicocca, 20126 Milan, Italy; and [j]Courant Institute of Mathematical Sciences, New York University, New York, NY 10003

Edited by Michael Wigler, Cold Spring Harbor Laboratory, Cold Spring Harbor, NY, and approved May 16, 2016 (received for review October 13, 2015)

The genomic evolution inherent to cancer relates directly to a renewed focus on the voluminous next-generation sequencing data and machine learning for the inference of explanatory models of how the (epi)genomic events are choreographed in cancer initiation and development. However, despite the increasing availability of multiple additional -omics data, this quest has been frustrated by various theoretical and technical hurdles, mostly stemming from the dramatic heterogeneity of the disease. In this paper, we build on our recent work on the "selective advantage" relation among driver mutations in cancer progression and investigate its applicability to the modeling problem at the population level. Here, we introduce PiCnIc (Pipeline for Cancer Inference), a versatile, modular, and customizable pipeline to extract ensemble-level progression models from cross-sectional sequenced cancer genomes. The pipeline has many translational implications because it combines state-of-the-art techniques for sample stratification, driver selection, identification of fitness-equivalent exclusive alterations, and progression model inference. We demonstrate PiCnIc's ability to reproduce much of the current knowledge on colorectal cancer progression as well as to suggest novel experimentally verifiable hypotheses.

cancer evolution | selective advantage | Bayesian structural inference | next generation sequencing | causality

Since the late 1970s evolutionary dynamics, with its interplay between variation and selection, has progressively provided the widely accepted paradigm for the interpretation of cancer emergence and development (1–3). Random alterations of an organism's (epi)genome can sometimes confer a functional selective advantage* to certain cells, in terms of adaptability and ability to survive and proliferate. Because the consequent clonal expansions are naturally constrained by the availability of resources (metabolites, oxygen, etc.), further mutations in the emerging heterogeneous tumor populations are necessary to provide additional fitness of different kinds that allow survival and proliferation in the unstable microenvironment. Such further advantageous mutations will eventually allow some of their subclones to outgrow the competing cells, thus enhancing a tumor's heterogeneity as well as its ability to overcome future limitations imposed by the rapidly exhausting resources. Competition, predation, parasitism, and cooperation have been in fact theorized as copresent among cancer clones (4).

In the well-known vision of Hanahan and Weinberg (5, 6), the phenotypic stages that characterize this multistep evolutionary process are called hallmarks. These can be acquired by cancer cells in many possible alternative ways, as a result of a complex biological interplay at several spatiotemporal scales that is still only partially deciphered (7). In this framework, we distinguish "alterations" driving the hallmark acquisition process (i.e., drivers) by activating oncogenes or inactivating tumor suppressor genes, from those that are transferred to subclones without increasing their fitness (i.e., passengers) (8). Driver identification is a modern challenge of cancer biology, because distinct cancer types exhibit very different combinations of drivers, some cancers display mutations in hundreds of genes (9), and the majority of drivers are mutated at low frequencies ("long tail" distribution), hindering their detection only from the statistics of the recurrence at the population level (10).

Cancer clones harbor distinct types of alterations. The somatic (or genetic) ones involve either few nucleotides or larger chromosomal regions. They are usually cataloged as mutations, that is, single nucleotide or structural variants at multiple scales (insertions, deletions, inversions, or translocations)—of which only some are detectable as copy number alterations (CNAs), most prevalent in many tumor types (11). Also epigenetic alterations, such as DNA methylation and chromatin reorganization, play a key role in the process (12). The overall picture is confounded by factors such as genetic instability (13), tumor–microenvironment interplay (14, 15), and the influence of spatial organization and tissue specificity on tumor development (16).†

Significantly, in many cases, distinct driver alterations can damage in a similar way the same functional pathway, leading to the acquisition of new hallmarks (17–21). Such alterations individually provide an equivalent fitness gain to cancer cells, because any additional alteration hitting the same pathway would provide no further selective advantage. This dynamic results in groups of driver alterations that form mutually exclusive patterns across tumor samples from different patients (i.e., the sets of alterations that are involved in the same pathways tend not to occur mutated together). This phenomenon has significant translational consequences.

Significance

A causality-based machine learning Pipeline for Cancer Inference (PiCnIc) is introduced to infer the underlying somatic evolution of ensembles of tumors from next-generation sequencing data. PiCnIc combines techniques for sample stratification, driver selection, and identification of fitness-equivalent exclusive alterations to exploit an algorithm based on Suppes' probabilistic causation. The accuracy and translational significance of the results are studied in detail, with an application to colorectal cancer. The PiCnIc pipeline has been made publicly accessible for reproducibility, interoperability, and future enhancements.

Author contributions: G.C., A.G., D.R., L.D.S., G.M., V.M., M.A., and B.M. designed research; G.C., A.G., D.R., and L.D.S. performed research; G.C., A.G., D.R., R.S.-P., L.D.S., and B.M. analyzed data; and G.C., A.G., D.R., R.S.-P., V.M., M.A., and B.M. wrote the paper.

The authors declare no conflict of interest.

This article is a PNAS Direct Submission.

[1]To whom correspondence should be addressed. Email: giulio.caravagna@ed.ac.uk.

This article contains supporting information online at www.pnas.org/lookup/suppl/doi:10.1073/pnas.1520213113/-/DCSupplemental.

*For this and other technical terms commonly used in the statistics and cancer biology communities we provide a glossary in the *SI Appendix*.

†We mention that much attention has been recently cast on newly discovered cancer genes affecting global processes that are apparently not directly related to cancer development, such as cell signaling, chromatin and epigenomic regulation, RNA splicing, protein homeostasis, metabolism, and lineage maturation (10).

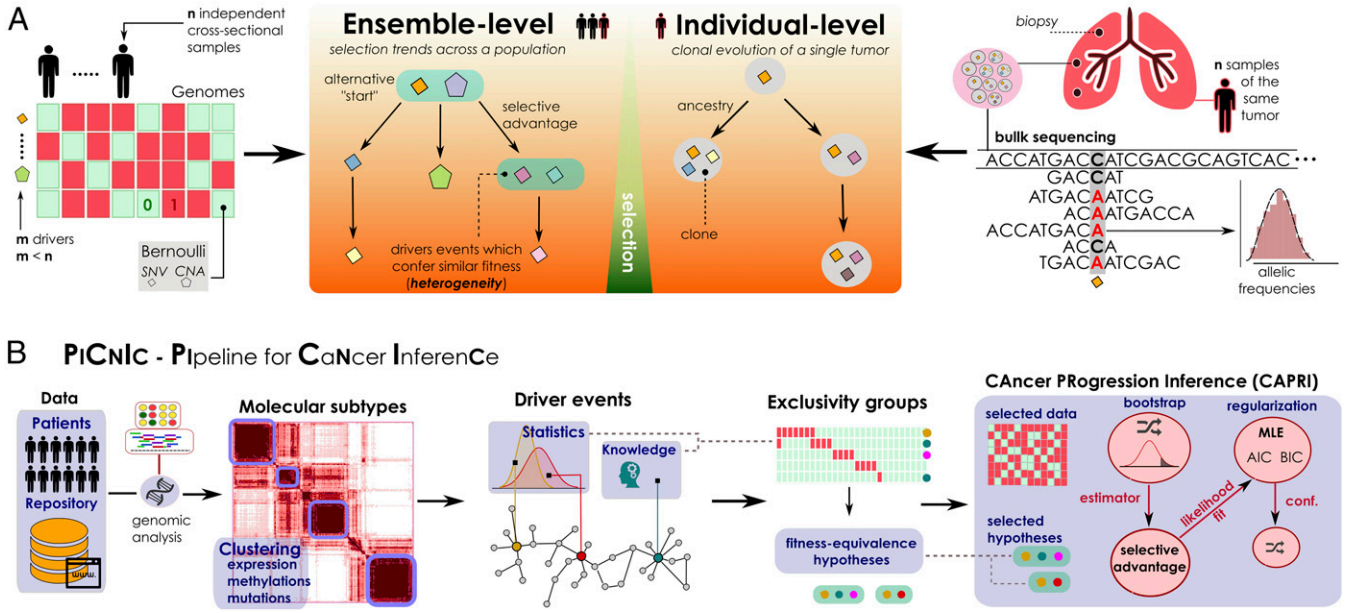

Fig. 1. (*A*) Problem statement. (*A*, *Left*) Inference of ensemble-level cancer progression models from a cohort of *n* independent patients (cross-sectional). By examining a list of somatic mutations or CNAs per patient (0/1 variables) we infer a probabilistic graphical model of the temporal ordering of fixation and accumulation of such alterations in the input cohort. Sample size and tumor heterogeneity complicate the problem of extracting population-level trends, because this requires accounting for patients' specificities such as multiple starting events. (*A*, *Right*) For an individual tumor, its clonal phylogeny and prevalence is usually inferred from multiple biopsies or single-cell sequencing data. Phylogeny-tree reconstruction from an underlying statistical model of reads coverage or depths estimates alterations' prevalence in each clone, as well as ancestry relations. This problem is mostly worsened by the high intratumor heterogeneity and sequencing issues. (*B*) The PiCnIc pipeline for ensemble-level inference includes several sequential steps to reduce tumor heterogeneity, before applying the CAPRI (40) algorithm. Available mutation, expression, or methylation data are first used to stratify patients into distinct tumor molecular subtypes, usually by exploiting clustering tools. Then, subtype-specific alterations driving cancer initiation and progression are identified with statistical tools and on the basis of prior knowledge. Next is the identification of the fitness-equivalent groups of mutually exclusive alterations across the input population, again done with computational tools or biological priors. Finally, CAPRI processes a set of relevant alterations within such groups. Via bootstrap and hypothesis testing, CAPRI extracts a set of "selective advantage relations" among them, which is eventually narrowed down via maximum likelihood estimation with regularization (with various scores). The ensemble-level progression model is obtained by combining such relations in a graph, and its confidence is assessed via various bootstrap and cross-validation techniques.

An immediate challenge posed by this state of affairs is the dramatic heterogeneity of cancer, both at the intertumor and at the intratumor levels (22). The former manifests as different patients with the same cancer type that can display few common alterations. This observation led to the development of techniques to stratify tumors into subtypes with different genomic signatures, prognoses, and response to therapy (23). The latter form of heterogeneity refers to the observed genotypic and phenotypic variability among the cancer cells within a single neoplastic lesion, characterized by the coexistence of more than one cancer clones with distinct evolutionary histories (24).

Cancer heterogeneity poses a serious problem from the diagnostic and therapeutic perspective because, for instance, it is now acknowledged that a single biopsy might not be representative of other parts of the tumor, hindering the problem of devising effective treatment strategies (4). Therefore, presently the quest for an extensive etiology of cancer heterogeneity and for the identification of cancer evolutionary trajectories is central to cancer research, which attempts to exploit the massive amount of sequencing data available through public projects such as The Cancer Genome Atlas (TCGA) (25).

Such projects involve an increasing number of cross-sectional (epi)genomic profiles collected via single biopsies of patients with various cancer types, which might be used to extract trends of cancer evolution across a population of samples.[‡] Higher-resolution data such as multiple samples collected from the same tumor (24), as well as single-cell sequencing data (26), might be complementarily used to face the same problem within a specific patient. However, the lack of public data coupled to the problems of accuracy and reliability currently prevents a straightforward application (27).

These different perspectives lead to the different mathematical formulations of the problem of inferring a cancer progression model from genomic data and a need for versatile computational tools to analyze data reproducibly—two intertwined issues examined at length in this paper (28). Indeed, such models and tools can be focused either on characteristics of a population, that is, ensemble-level, or on multiple clonality in a single patient. In general, both problems deal with understanding the temporal ordering of somatic alterations accumulating during cancer evolution but use orthogonal perspectives and different input data; see Fig. 1 for a comparison. This paper proposes a computational approach to efficiently deal with various aspects of the problem at a patient population level, for now.

Ensemble-Level Cancer Evolution

It is thus desirable to extract a probabilistic graphical model explaining the statistical trend of accumulation of somatic alterations in a population of *n* cross-sectional samples collected from patients diagnosed with a specific cancer. To normalize against the experimental conditions in which tumors are sampled, we only consider the list of alterations detected per sample—thus, as 0/1 Bernoulli random variables.

Much of the difficulty lies in estimating the true and unknown trends of selective advantage among genomic alterations in the data from such observations. This hurdle is not unsurmountable, if we constrain the scope to only those alterations that are persistent across tumor evolution in all subclonal populations, because it yields a consistent model of a temporal ordering of mutations. Therefore, epigenetic and trascriptomic states, such as hyper- and

[‡]At the time of this writing, in TCGA, sample sizes per cancer type are in the order of a few hundred. Such numbers are expected to increase in the near future, with a clear benefit for all the statistical approaches to analyze cancer data that currently lack a proper background of data.

PiCnIc Pipeline for Cancer Inference		MOTIVATION	INPUT DATA *					COMPUTATIONAL OPTIONS AND PRIOR KNOWLEDGE ⌘		EXPECTED OUTPUT AND ACTION TO EXECUTE	
			Mutations	Copy Number	Expression	Mehtylations	Other				
1	Cohort subtyping	*Determine molecular subtypes likely to progress through different trajectories*	✓	✓	✓			Non-negative Matrix Factorization (NMF), k-Means, Gaussian Mixtures, Hierarchical/Spectral Clustering, Network Based Stratification (NBS)	Biomarkers (cell types, known mutations, ….), Clinical Annotations (Mutation Status, Chromosomal Stability, …)	*Stratified samples (clusters)*	**Split the cohort according to each cluster**
2	Events selection	*Select a subset of alterations likely to drive progression*	✓	✓	✓			MutSigCV, OncodriveFM, OncodriveCLUST, MuSiC, Oncodrive-CIS, Intogen	Known cancer oncogenes and tumor suppressors, known pathways	*A rank of genes and their alterations*	**In each cluster, restrict to consider only driver events**
3	Groups detection	*Select groups of alterations which should be examined together*	✓	✓	✓			Ratio test, RME, MEMO, MUTEX, Dendrix, MDPFinder, Multi-Dendrix, CoMEt, MEGSA, ME test	Known pathway genes with alternative but fitness-equivalent status, or co-occurrently altered	*Groups satysifying certain statistics (e.g., exclusivity)*	**For each cluster, for each of its groups, create a logical formula consistent with the statistic**
4	Model Inference	*Select the Graphical Model which explains best the data*	✓	✗	✗			CAPRI ★, CAPRESE, Oncotrees, Distance-based, Mixtures, CBN, Resic, BML		*One progression model per subtype*	**Validate statistically or experimentally each one of the inferred models**

* Data marked as ✗ can be used when it is persistent (i.e., do not revert back to their original state) during tumor progression. Other: data not common to most tumor types such as fusions or partial tandem duplication.
⌘ Not all tools support all the data that is theoretically usable for a certain step.
★ CAPRI is the only algorithm to exploit knowledge provided by step 3 via logical formulas hypotheses-testing. Oncotrees, Distance-based, Mixtuers and CAPRESE are constrained to infer at most tree-models of progression.

Fig. 2. The PiCnIc pipeline. We do not provide a unique all-encompassing rationale to instantiate PiCnIc because all steps refer to a research area currently under development, where the optimal approach is often dependent on the type of data available and prior knowledge about the cancer under study. References are provided for each tool that can be used to instantiate PiCnIc: NMF (61), *k*-means, Gaussian mixtures, hierarchical/spectral clustering (62), NBS (66), MutSigCV (68), OncodriveFM (69), OncodriveCLUST (70), MuSiC (71), Oncodrive-CIS (72), Intogen (73), Ratio (74), RME (75), MEMO (76), MUTEX (77), Dendrix (78), MDPFinder (79), Multi-Dendrix (80), CoMEt (81), MEGSA (82), ME (83), CAPRI (40), CAPRESE (39), Oncotrees (31, 33), distance-based (32), mixtures (34), CBN (35, 36), Resic (37), and BML (38).

hypomethylations or over- and underexpression, could only be used, provided that they are persistent through tumor development (29).

Historically, the linear model of colorectal tumor progression by Vogelstein is an instance of an early solution to the cancer progression problem (30). That approach was later generalized to accommodate tree models of branched evolution (31–34) and later further generalized to the inference of directed acyclic graph models, with several distinct strategies (35–38). We contributed to this research program with the Cancer Progression Extraction with Single Edges (CAPRESE) and the Cancer Progression Inference (CAPRI) algorithms, which are currently implemented in TRONCO, an open-source R package for translational oncology available in standard repositories (39–41). Both techniques rely on Suppes' theory of probabilistic causation to define estimators of selective advantage (42), are robust to the presence of noise in the data, and perform well even with limited sample sizes. The former algorithm exploits shrinkage-like statistics to extract a tree model of progression, and the latter combines bootstrap and maximum likelihood estimation with regularization to extract general directed acyclic graphs that capture branched, independent, and confluent evolution. Both algorithms represent the current state-of-the-art approach to this problem, because they outperform others in speed, scale, and predictive accuracy.

Clonal Architecture in Individual Patients

A closely related problem addresses the detection of clonal signatures and their prevalence in individual tumors, a problem complicated by intratumor heterogeneity.

Even though this phylogenetic version of the progression inference problem naturally relies on data produced from single-cell sequencing assays (43, 44), the majority of approaches still make use of bulk sequencing data, usually from multiple biopsies of the same tumors (24, 45). Indeed, several approaches try to extract the clonal signature of single tumors from allelic imbalance proportions, a problem made difficult because sequenced samples usually contain a large number of cells belonging to a collection of subclones resulting from the complex evolutionary history of the tumor (46–55).

We keep the current work focused on the inference of progression models at the ensemble level.

The PiCnIc Pipeline

We report on the design, development, and evaluation of the Pipeline for Cancer Inference (PiCnIc) to extract ensemble-level cancer progression models from cross-sectional data (Fig. 1). PiCnIc is versatile, modular, and customizable; it exploits state-of-the-art data processing and machine learning tools to do the following:

i) identify tumor subtypes and then in each subtype;
ii) select (epi)genomic events relevant to the progression;
iii) identify groups of events that are likely to be observed as mutually exclusive;
iv) infer progression models from groups and related data and annotate them with associated statistical confidence.

All these steps are necessary to minimize the confounding effects of intertumor heterogeneity, which are likely to lead to wrong results when data are not appropriately preprocessed.[§]

In each stage of PiCnIc different techniques can be used, alternatively or jointly, according to specific research goals, input data, and cancer type. Prior knowledge can be easily accommodated into our pipeline, as well as the computational tools discussed in the following subsections and summarized in Fig. 2. The rationale is similar in spirit to workflows implemented by consortia such as TCGA to analyze huge populations of cancer samples (56, 57). One of the main novelties of our approach is the exploitation of groups of exclusive alterations as a proxy to detect fitness-equivalent trajectories of cancer progression. This strategy is only feasible by the hypothesis-testing features of the recently developed CAPRI algorithm, an algorithm uniquely addressing this crucial aspect of the ensemble-level progression inference problem (40).

In *Results* we study in detail a specific use case for the pipeline, processing colorectal cancer (CRC) data from TCGA, where it is able to rediscover much of the existing body of knowledge about CRC progression. Based on the output of this pipeline,

[§]The genuine selectivity relationship sought to be inferred are subject to the vagaries of Simpson's paradox; it can change, or worst reverse, when we try to infer them from data not suitably preprocessed. This effect (due to such paradox) manifests as data are sampled from a highly heterogenous mixture of populations of cells (40). PiCnIc uses various mechanisms to avoid these pitfalls. In this context, it should be pointed out that input bulk sequencing data suffers also from intratumor heterogeneity issues, which are unfortunately intrinsic to the technology.

we also propose several previously unidentified experimentally verifiable hypotheses.

Reducing Intertumor Heterogeneity by Cohort Subtyping. In general, for each of n tumors (patients) we assume relevant (epi)genetic data to be available. We do not put constraints on data gathering and selection, leaving the user to decide the appropriate "resolution" of the input data. For instance, one might decide whether somatic mutations should be classified by type or by location, or aggregated. Or, one might decide to lift focal CNAs to the lower resolution of cytobands or full arms [e.g., in a kidney cancer cohort where very long CNAs are more common than focal events (58)]. These choices depend on data and on the overall understanding of such alterations and their functional effects for the cancer under study, and no single all-encompassing rationale may be provided.

With these data at hand, we might wish to identify cancer subtypes in the heterogeneous mixture of input samples. In some cases the classification can benefit from clinical biomarkers, such as evidences of certain cell types (59), but in most cases we will have to rely on multiple clustering techniques at once (see, e.g., refs. 56 and 57). Many common approaches cluster expression profiles (60), often relying on nonnegative matrix factorization techniques (61) or earlier approaches such as k-means, Gaussian mixtures, or hierarchical/spectral clustering (see the review in ref. 62). For glioblastoma and breast cancer, for instance, mRNA expression subtypes provide good correlation with clinical phenotypes (63–65). However, this stratification strategy is not always applicable [e.g., in CRC such clusters mismatch with survival and chemotherapy response (63)]. Clustering of full exome mutation profiles or smaller panels of genes might be an alternative, as was shown for ovarian, uterine, and lung cancers (66, 67).

Using pipelines such as PiCnIc we expect that the resulting subtypes will be routinely investigated, eventually leading to distinct progression models characteristic of the population-level trends of cancer initiation and progression.

Selection of Driver Events. In subtype detection, it becomes easier to find similarities across input samples when more alterations are available, because features selection gains precision. In progression inference, instead, one wishes to focus on $m \ll n$ driver alterations, which ensures also an appropriate statistical ratio between sample size (n, here the subtype size) and problem dimension (m).

Multiple tools filter out driver from passenger mutations. MutSigCV identifies drivers mutated more frequently than background mutation rate (68). OncodriveFM avoids such estimation but looks for functional mutations (69). OncodriveCLUST scans mutations clustering in small regions of the protein sequence (70). MuSiC uses multiple types of clinical data to establish correlations among mutation sites, genes, and pathways (71). Some other tools search for driver CNAs that affect protein expression (72). All these approaches use different statistical measures to estimate signs of positive selection, and we suggest using them in an orchestrated way, as done by platforms such as Intogen (73).

We anticipate that such tools will run independently on each subtype, because driver genes will likely differ across them, mimicking the different molecular properties of each group of samples; also, lists of genes produced by these tools might be augmented with prior knowledge about tumor suppressors or oncogenes.

Fitness Equivalence of Exclusive Alterations. When working at the ensemble level, identification of "groups of mutually exclusive" alterations is crucial to derive a correct inference. This step of PiCnIc is another attempt to resolve part of the intertumor heterogeneity, because such alterations could lead to the same phenotype (i.e., hence resulting in "equivalent" in terms of progression), despite being genotypically "alternative" (i.e., exclusive across the input cohort). This information shall be used to detect alternative routes to cancer progression that capture the specificities of individual patients.

A plethora of recent tools can be used to detect groups of fitness equivalent alterations, according to the data available for each subtype: greedy approaches (74, 75) or their optimizations, such as MEMO, which constrain search-space with network priors (76). This strategy is further improved in MUTEX, which scans mutations and focal CNAs for genes with a common downstream effect in a curated signaling network and selects only those genes that significantly contributes to the exclusivity pattern (77). Other tools such as Dendrix, MDPFinder, Multi-Dendrix, CoMEt, MEGSA, or ME use advanced statistics or generative approaches without priors (78–83).

In such groups, we distinguish between hard and soft forms of exclusivity, the former assuming strict exclusivity among alterations, with random errors accounting for possible overlaps (i.e., the majority of samples do not share alterations from such groups), the latter admitting cooccurrences (i.e., some samples might have common alterations, within a group) (77).

CAPRI is currently the only algorithm that incorporates this type of information in inferring a model. Each of these groups is in fact associated with a "testable hypothesis" written in the well-known language of propositional Boolean formulas.[¶] Consider the following example: We might be informed that *APC* and *CTNNB1* mutations show a trend of soft exclusivity in our cohort (i.e., some samples harbor both mutations), but the majority just one of the two mutated genes. Because such mutations lead to β-catenin deregulation (the phenotype), we might wonder whether such a state of affairs could be responsible for progression initiation in the tumors under study. An affirmative response would equate, in terms of progression, the two mutations. To test this hypothesis, one may spell out formula *APC* ∨ *CTNNB1* to CAPRI, which means that we are suggesting to the inference engine that, besides the possible evolutionary trajectories that might be inferred by looking at the two mutations as independent, trajectories involving such a "composite" event shall be considered as well. It is then up to CAPRI to decide which, of all such trajectories, is significant, in a statistical sense.

In general, formulas allow users to test general hypotheses about complex model structures involving multiple genes and alterations. These are useful in many cases: for instance, where we are processing samples that harbor homozygous losses or inactivating mutations in certain genes (i.e., equally disruptive genomic events), or when we know in advance that certain genes are controlling the same pathway, and we might speculate that a single hit in one of those decreases the selection pressure on the others. We note that, with no hypothesis, a model with such alternative trajectories cannot be analyzed, due to various computational limitations inherent to the inferential algorithms (see ref. 40).

From a practical point of view, CAPRI's formulas/hypotheses-testing features "help" the inference process but do not "force" it to select a specific model (i.e., the inference is not biased). In this sense, the trajectories inferred by examining these composite model structures (i.e., the formulas) are not given any statistical advantage for inclusion in the final model. However, despite a natural temptation to generate as many hypotheses as possible, it is prudent to always limit the number of hypotheses according to the number of samples and alterations. Note that this approach can also be extended to accommodate, for instance, cooccurrent alterations in significantly mutated subnetworks (84, 85).

Progression Inference and Confidence Estimation. We use CAPRI to reconstruct cancer progression models of each identified molecular subtype, provided that there exist a reasonable list of driver events and the groups of fitness-equivalent exclusive alterations. Because currently CAPRI represents the state of the art, and supports complex formulas for groups of alterations detected in the earlier PiCnIc step, it was well-suited for the task.

CAPRI's input is a binary $n \times (m+k)$ matrix $\mathbf{M}$ with n samples (a subtype size), m driver alteration events (0/1 Bernoulli

[¶]There, logical connectives such as ⊕ (the logical "xor") act as a proxy for hard exclusivity, and ∨ (the logical "disjunction") for soft exclusivity. Besides from exclusivity groups, other connectives such as logical conjunction can be used.

random variables), and k testable formulas. Each sample in $\mathbf{M}$ is described by a binary sequence: the 1's denote the presence of alterations. CAPRI first performs a computationally fast scan of $\mathbf{M}$ to identify a set $\mathcal{S}$ of plausible selective advantage relations among the driver alterations and the formulas; then, it reduces $\mathcal{S}$ to the most relevant ones, $\hat{\mathcal{S}} \subset \mathcal{S}$. Each relation is represented as an edge connecting drivers/formulas in a graphical model, which shall be termed the Suppes–Bayes causal network. This network represents the joint probability distribution[#] of observing a set of driver alterations in a cancer genome, subject to constraints imposed by Suppes' probabilistic causation formalism (42).

Set $\mathcal{S}$ is built by a statistical procedure. Among any pair of input drivers/formulas x and y, CAPRI postulates that $x \to y \in \mathcal{S}$ could be a selective advantage relation with "x selecting for y" if it estimates that two conditions hold:

i) "x is earlier than y";
ii) "x's presence increases the probability of observing y."

Such claims, grounded in Suppes' theory of probabilistic causation, are expressed as inequalities over marginal and conditional distributions of x and y. These are assessed via a standard Mann–Withney U test after the distributions are estimated from a reasonable number (e.g., 100) of nonparametric bootstrap resamples of $\mathbf{M}$ (*SI Appendix*). CAPRI's increased performance over existing methods can be motivated by the reduction of the state space within which models are searched, via $\mathcal{S}$.

Optimization of $\mathcal{S}$ is central to our tolerance to false positives and negatives in $\hat{\mathcal{S}}$. We would like to select only the minimum number of relations that are true and statistically supported and build our model from those. CAPRI's implementation in TRONCO (41) selects a subset by optimizing a score function that assigns to a model a real number equal to its log likelihood (probability of generating data for the model) minus a penalty term for model complexity—a regularization term increasing with $\hat{\mathcal{S}}$'s size, and hence penalizing overly complex models. It is a standard approach to avoid overfitting and usually relies on the Akaike or the Bayesian information criterion (AIC or BIC) as regularizers. Both scores are approximately correct; AIC is more prone to overfitting but also likely to provide good predictions from data and is better when false negatives are more misleading than positive ones. BIC is more prone to underfitting errors, thus more parsimonious and better in the opposite direction. As is often done, we suggest approaches that combine but distinguish which relations are selected by BIC versus AIC. Details of the algorithm are provided in the *SI Appendix*.

Statistical Confidence of a Model. In vitro and in vivo experiments provide the most convincing validation for the newly suggested selective advantage relations and hypotheses, such a validation scheme is out of reach in some cases.

Nonetheless, statistical validation approaches can be used almost universally to assess the confidence of edges, parent sets, and whole models, either via hypothesis testing or bootstrap and cross-validation scores for graphical models. We briefly discuss approaches that are implemented in TRONCO and refer to the *SI Appendix* for additional details.

First, CAPRI builds $\mathcal{S}$ by computing two P values per edge, for the confidence in conditions i and ii. In addition, for each edge $x \to y$, it computes a third P value via hypergeometric testing against the hypothesis that the cooccurrence of x and y is due to chance. These P values measure confidence in the direction of each edge and the amount of statistical dependence among x and y.

Second, for each model inferred with CAPRI we can estimate (a posteriori) how frequently our edges would be retrieved if we resample from our data (nonparametric bootstrap), or from the model itself, assuming its correctness (parametric bootstrap) (86). Also, we can measure the bias in CAPRI's construction of $\mathcal{S}$ due to the random procedure which estimates the distributions in conditions i and ii (statistical bootstrap).

Third, scores can be computed to quantify the consistency for the model against bias in the data and models. For instance, nonexhaustive k-fold cross-validation can be used to compute the entropy loss for the whole model, and the prediction and posterior classification errors for each edge or parent set (87).

Results

Evolution in a Population of Microsatellite Unstable/Microsatellite Stable Colorectal Tumors. It is common knowledge that CRC is a heterogeneous disease comprising different molecular entities. Indeed, it is currently accepted that colon tumors can be classified according to their global genomic status into two main types: microsatellite unstable tumors (MSI), further classified as high or low, and microsatellite stable (MSS) tumors (also known as tumors with chromosomal instability). This taxonomy plays a significant role in determining pathologic, clinical, and biological characteristics of CRC tumors (88). Regarding molecular progression, it is also well established that each subtype arises from a distinctive molecular mechanism. Whereas MSS tumors generally follow the classical adenoma-to-carcinoma progression described in the seminal work by Vogelstein and Fearon (89), MSI tumors result from the inactivation of DNA mismatch repair genes such as *MLH-1* (90).

With the aid of the TRONCO package, we instantiated PiCnIc to process colorectal tumors freely available through the TCGA project COADREAD ("Human Colon and Rectal Cancer") (56) (*SI Appendix*, Fig. S1) and inferred models for the MSS and MSI-HIGH tumor subtypes (shortly denoted MSI) annotated by the consortium. In doing so, we used a combination of background knowledge produced by TCGA and new computational predictions; to a different degree, some knowledge comes from manual curation of data and other from tools mentioned in PiCnIc's description (Fig. 2). Data and exclusivity groups for MSI tumors are shown in Fig. 3; the analogous information for MSS tumors is provided as *SI Appendix*, Figs. S4 and S5.

For the models inferred, which are shown in Figs. 4 and 5, we evaluated various forms of statistical confidence measured as P values, bootstrap scores (in what follows, npb denotes nonparametric bootstrap and the closer to 100 the better), and cross-validation statistics reported in the *SI Appendix* and Dataset S1. Many of the postulated selective advantage relations (i.e., model edges) have very strong statistical support for COADREAD samples, although events with similar marginal frequency may lead to ambiguous imputed temporal ordering (i.e., the edge direction). In general, we observed that overall the estimates are slightly better in the MSS cohort (entropy loss <1% versus 3.8%), which is expected given the difference in sample size of the two datasets (152 versus 27 samples); see the *SI Appendix* for details.

Interpretation of the Models. Our models capture the well-known features distinguishing MSS and MSI tumors: for the former, *APC*, *KRAS*, and *TP53* mutations as primary events together with chromosomal aberrations; for the latter, *BRAF* mutations and lack of chromosomal alterations. Of all 33 driver genes, 15 are common to both models (e.g., *APC*, *BRAF*, *KRAS*, *NRAS*, *TP53*, and *FAM123B*, among others, mapped to pathways such as WNT, MAPK, apoptosis, or activation of T-cell lymphocytes), although in different relationships (position in the model), whereas new (previously unimplicated) genes stood out from our analysis and deserve further research.

MSS. In agreement with the known literature, in addition to *KRAS*, *TP53*, and *APC* as primary events, we identify *PTEN* as a

[#]Technically, for a set of m alterations modeled by variables $\mathbf{x}_1, \ldots, \mathbf{x}_m$, such a network is a graphical model representing the factorization of the joint distribution—$\mathcal{P}(\mathbf{x}_1, \ldots \mathbf{x}_m)$—of observing any of the alterations in a genome (i.e., $\mathbf{x}_i = 1$). This factorization is made compact as the model encodes the statistical dependencies in its structure via $\mathcal{P}(\mathbf{x}_1, \ldots, \mathbf{x}_m) = \prod_{i=1}^{m} \mathcal{P}(\mathbf{x}_i | \pi_i)$, where $\pi_i = \{\mathbf{x}_j | \mathbf{x}_j \to \mathbf{x}_i \in \hat{\mathcal{S}}\}$ are the "parents" of the i-th node. These are those from which the presence of the i-th alteration is predicted. In our approach these edges are the pictorial representation of the selective advantage relations where the alterations in π_i select for $\mathbf{x}_i$.

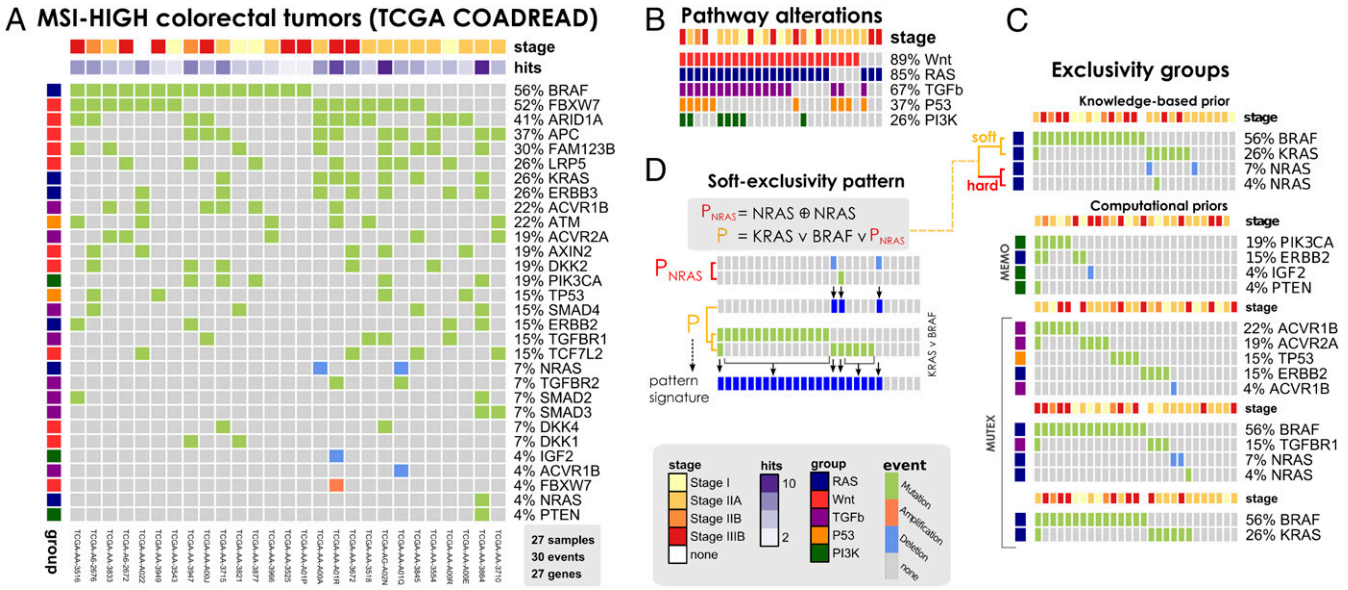

Fig. 3. (*A*) MSI-HIGH colorectal tumors from the TCGA COADREAD project (56), restricted to 27 samples with both somatic mutations and high-resolution CNA data available and a selection out of 33 driver genes annotated to WNT, RAS, PI3K, TGF-β, and P53 pathways. This dataset is used to infer the model in Fig. 5. (*B*) Mutations and CNAs in MSI-HIGH tumors mapped to pathways confirm heterogeneity even at the pathway level. (*C*) Groups of mutually exclusive alterations were obtained from ref. 56—which run the MEMO (76) tool—and by MUTEX (77) tool. In addition, previous knowledge about exclusivity among genes in the RAS pathway was exploited. (*D*) A Boolean formula input to CAPRI tests the hypothesis that alterations in the RAS genes *KRAS*, *NRAS*, and *BRAF* confer equivalent selective advantage. The formula accounts for hard exclusivity of alterations in *NRAS* mutations and deletions, jointly with soft exclusivity with *KRAS* and *NRAS* alterations.

late event in carcinogenesis, as well as *NRAS* and *KRAS* converging in *IGF2* amplification, the former being "selected by" *TP53* mutations (npb 49%), the latter "selecting for" *PIK3CA* mutations (npb 81%). The leftmost portion of the model links many WNT genes, in agreement with the observation that multiple concurrent lesions affecting such pathway confer selective advantage. In this respect, our model predicts multiple routes for the selection of alterations in *SOX9* gene, a transcription factor known to be active in colon mucosa (91). Its mutations are directly selected by *APC*/*CTNNB1* alterations (although with low npb score), by *ARID1A* (npb 34%), or by *FBXW7* mutations (npb 49%), an early mutated gene that both directly, and in a redundant way via *CTNNB1*, relates to *SOX9*. The *SOX* family of transcription factors have emerged as modulators of canonical WNT/β-catenin signaling in many disease contexts (92). Also interestingly, *FBXW7* has been previously reported to be involved in the malignant transformation from adenoma to carcinoma (93). The rightmost part of the model involves genes from various pathways, and outlines the relation between *KRAS* and the PI3K pathway. We indeed find selection of *PIK3CA* mutations by *KRAS* ones, as well as selection of the whole MEMO module (npb 64%), which is responsible for the activation of the PI3K pathway (56). *SMAD4* proteins relate either to *KRAS* (npb 34%) and *FAM123B* (through *ATM*) and *TCF7L2* converge in *DKK2* or *DKK4* (npb 81, 17, and 34%).

MSI-HIGH. In agreement with the current literature, *BRAF* is the most commonly mutated gene in MSI tumors (94). CAPRI predicted convergent evolution of tumors harboring *FBXW7* or *APC* mutations toward deletions/mutations of the *NRAS* gene (npb 21, 28, and 54%), as well as selection of *SMAD2* or *SMAD4* mutations by *FAM123B* mutations (npb 23 and 46%), for these tumors. Relevant to all MSI tumors seems again the role of the PI3K pathway. Indeed, a relation among *APC* and *PIK3CA* mutations was inferred (npb 66%), consistent with recent experimental evidences pointing at a synergistic role of these mutations, which cooccur in the majority of human CRCs (95). Similarly, we find consistently a selection trend among *APC* and the whole MEMO module (npb 48%). Interestingly, both mutations in *APC* and *ERBB3* select for *KRAS* mutations (npb 51 and 27%), which might point to interesting therapeutic implications. In contrast, mutations in *BRAF* mostly select for mutations in *ACVR1B* (npb 36%), a receptor that once activated phosphorylates SMAD proteins. It forms receptor complex with *ACVR2A*, a gene mutated in these tumors that selects for *TCF7L2* mutations (npb 34%). Tumors harboring *TP53* mutations are those selected by mutations in *AXIN2* (npb 32%), a gene implicated in WNT signaling pathway, and related to unstable gastric cancer development (96). Inactivating mutations in this gene are important, as it provides serrated adenomas with a mutator phenotype in the MSI tumorigenic pathway (97). Thus, our results reinforce its putative role as driver gene in these tumors.

By comparing these models we can find similarity in the prediction of a potential new early event for CRC formation, *FBXW7*, as other authors have recently described (93). This tumor suppressor is frequently inactivated in human cancers, yet the molecular mechanism by which it exerts its antitumor activity remains unexplained (98), and our models provide a previously unidentified hypothesis in this respect.

Discussion

This paper represents our continued exploration of the nature of somatic evolution in cancer and its translational exploitation through models of cancer progression, models of drug resistance (and efficacy), left- and right-censoring, sample stratification, and therapy design. Thus, this paper emphasizes the engineering and dissemination of production-quality computational tools as well as validation of its applicability via use cases carried out in collaboration with translational collaborators (e.g., CRC, analyzed jointly with epidemiologists currently studying the disease actively). As anticipated, we reasserted that the proposed model of somatic evolution in cancer not only supports the heterogeneity seen in tumor population but also suggests a selectivity/causality relation that can be used in analyzing (epi)genomic data and exploited in therapy design—which we introduced in our earlier work (39, 40). In this paper, we have introduced an open-source pipeline, PiCnIc, that minimizes the confounding effects arising

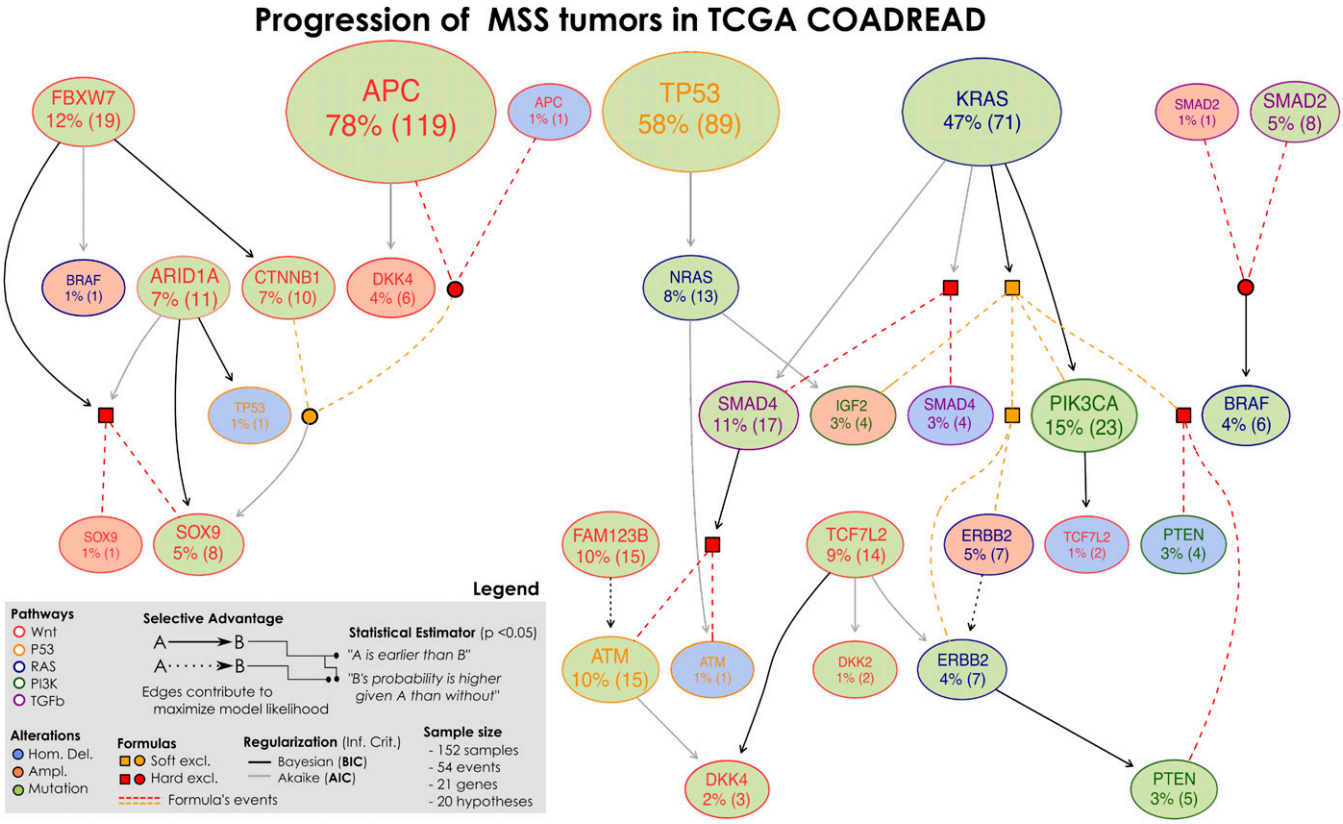

Fig. 4. Selective advantage relations inferred by CAPRI constitute MSS progression; the input dataset is given in *SI Appendix*, Figs. S4 and S5. Formulas written on groups of exclusive alterations (e.g., *SOX9* amplifications and mutations) are displayed in expanded form; their events are connected by dashed lines with colors representing the type of exclusivity (red for hard, orange for soft). Logical connectives are squared when the formula is selected and circular when the formula selects for a downstream node. For this model of MSS tumors in COADREAD we find strong statistical support for many edges (*P* values, bootstrap scores, and cross-validation statistics shown in the *SI Appendix*), as well as the overall model. This model captures both current knowledge about CRC progression—for example, selection of alterations in PI3K genes by the *KRAS* mutations (directed or via the MEMO group, with BIC)—as well as novel interesting testable hypotheses [e.g., selection of *SOX9* alterations by *FBXW7* mutations (with BIC)].

from intertumor heterogeneity, and we have shown that PiCnIc can be effective in extracting ensemble-level evolutionary trajectories of cancer progression.

When applied to a highly heterogeneous cancer such as CRC, PiCnIc was able to infer the role of many known events in CRC progression (e.g., *APC*, *KRAS*, or *TP53* in MSS tumors and *BRAF* in MSI tumors), confirming the validity of our approach.[‖] Interestingly, new players in CRC progression stand out from this analysis such as *FBXW7* or *AXIN2*, which deserve further investigation. In colon carcinogenesis, although each model identifies characteristic early mutations suggesting different initiation events, both models seem to converge in common pathways and functions such as WNT or MAPK.

However, both models have some clear distinctive features. Specific events in MSS include mutations in intracellular genes such as *CTNNB1* or in *PTEN*, a well-known tumor suppressor gene. On the contrary, specific mutations in MSI tumors appear in membrane receptors such as *ACVR1B*, *ACVR2A*, *ERBB3*, *LRP5*, *TGFBR1*, and *TGFBR2*, as well as in secreted proteins such as IGF2, possibly suggesting that such tumors need to disturb cell–cell and/or cell–microenvironment communication to grow. At the pathway level, genes exclusively appearing in the MSI progression model accumulate in specific pathways such as cytokine–cytokine receptor, endocytosis, and TGF-β signaling pathway. However, genes in MSS progression model are implicated in p53, mTOR, sodium transport, or inositol phosphate metabolism.

Our study also highlighted the translational relevance of the models that we can produce with PiCnIc (*SI Appendix*, Fig. S12). The evolutionary trajectories depicted by our models can, for instance, suggest previously uncharacterized phenotypes, help in finding biomarker molecules predicting cancer progression and therapy response, explain drug-resistant phenotypes, and predict metastatic outcomes. The logical structure of the formulas describing alterations with equivalent fitness (i.e., the exclusivity group) can also point to novel targets of therapeutic interventions. In fact, exclusivity groups that are found to have a role in the progression can be screened for synthetic lethality among such genes—thus explaining why we do not observe phenotypes where such alterations cooccur. In this sense, our models describe also such clonal signatures which, though theoretically possible, are not selected. We call such conspicuously absent phenotypes antihallmarks (100).

Our models have other applications to both computational and cancer research. Our models, as encoded by Suppes–Bayes causal networks, could be used as informative generative models for the genomic profiles for the cancer patients. In fact, as known in machine learning, such generative models are extremely useful in creating better representation of data in terms of, for instance, discriminative kernels, such as Fisher (101). In practice, this change of representations would allow framing common classification problems in the domain of our generative structures, that is, the models, rather than the data. As a consequence, it is possible to create a new class of more robust classification and prediction systems.

[‖]As a further investigation for CRC, we leave as future work to check whether the inferred progressions are also representative of other subtyping strategies for CRC, with particular reference to recent works that show marked interconnectivity between different independent classification systems coalescing into four consensus molecular subtypes (99).

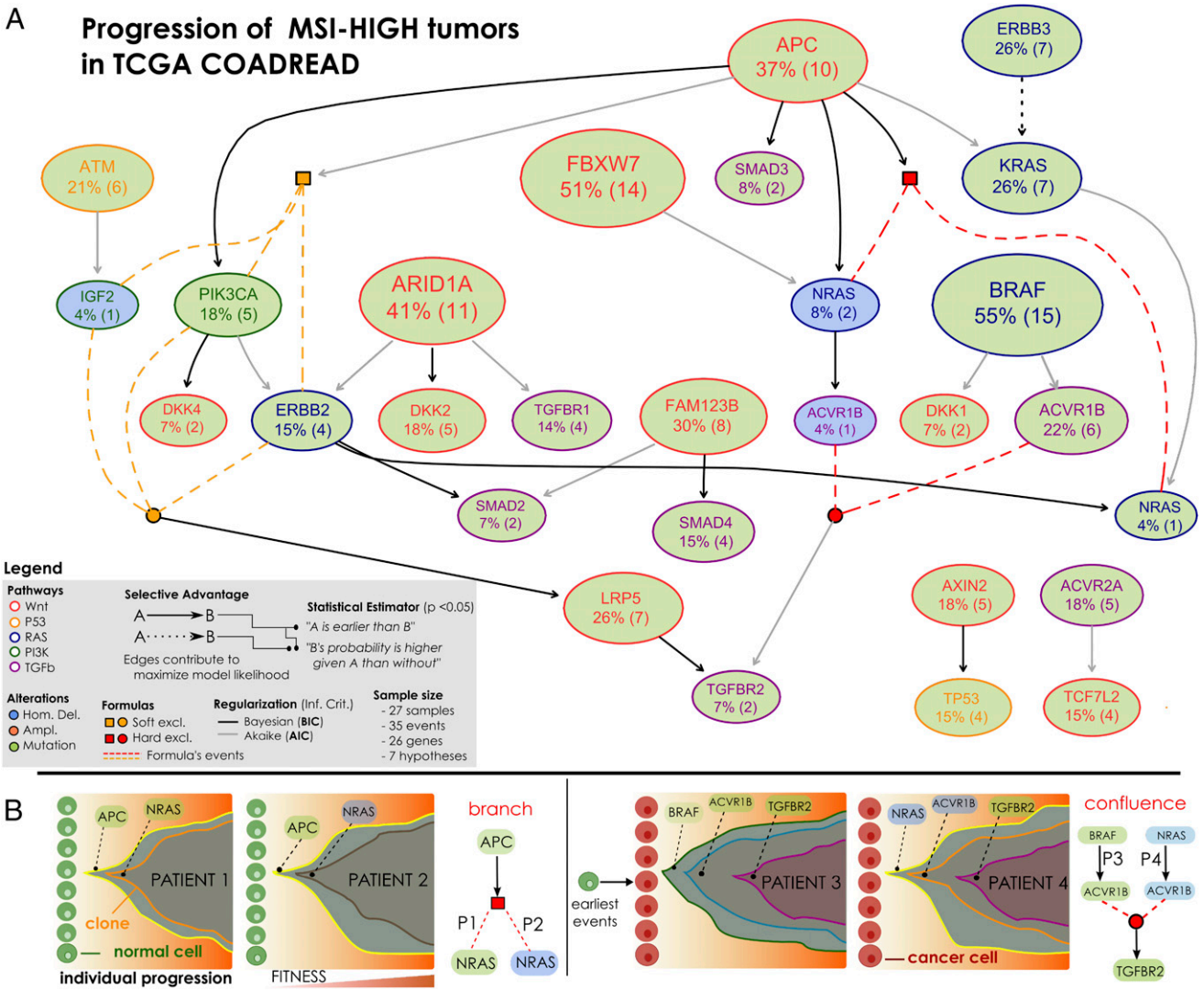

Fig. 5. (*A*) Selective advantage relations inferred by CAPRI constitute MSI-HIGH progression; the input dataset is given in Fig. 3. Formulas written on groups of exclusive alterations are expanded as in Fig. 4. For each relation, confidence is estimated as for MSS tumors and reported in the *SI Appendix*. In general, this model is supported by weaker statistics than MSS tumors—possibly because of this small sample size ($n = 27$). Still, we can find interesting relations involving *APC* mutations that select for *PIK3CA* ones (via BIC) as well as selection of the MEMO group (*ERBB2*/*PIK3CA* mutations or *IGF2* deletions) predicted by AIC. Similarly, we find a strong selection trend among mutations in *ERBB2* and *KRAS*, despite the fact that in this case the temporal precedence among those mutations is not disentangled because the two events have the same marginal frequencies (26%). (*B*) Branching and confluent evolutionary trajectories of clonal expansion inferred from the selective advantage relations implicit in the data. Such trajectories capture progression trends that are representative of alternative trajectories among patients, as driven by different types of genomic lesions. Note, that while the majority of the selectivity inferences are genuine, some of them could be spurious: e.g., the suggestion that *APC*-mutated clones shall enjoy expansion, up to acquisition of further selective advantage via mutations or homozygous deletions in *NRAS*. Nonetheless, the putative genuine selectivity relations need to be further validated: e.g., the suggestion that the clones of patients harbouring distinct alterations in *ACVR1B*—and different upstream events—will enjoy further selective advantage from mutation in the *TGFBR2* gene.

One may think of these representations as those bringing us closer to phenotypic (and causal) representation of the patient's tumor, replacing its genotypic (and mutational) representation. We suspect that such representations will improve the accuracy of measurement of the biological clocks dysregulated in cancer and critically needed to be measured to predict survival time, time to metastasis, time to evolution of drug resistance, and so on. We believe that these "phenotypic clocks" can be used immediately to direct the therapeutic intervention.

Clearly, applicability and reliability of techniques such as PiCnIc are very much dependent on the background of data available. At the time of this writing, the quality, quantity, and reliability of (epi) genomic data available (e.g., in public databases) is related to the ever-increasing computational and technological improvements characterizing the wide area of cancer genomics. Of similar importance is the availability of wet-laboratory technologies for model validation. Our recent work on SubOptical Mapping technology, for instance, points to the ability to cheaply and accurately characterize translocation, indels, and epigenomic modifications at the single-molecule and single-cell level (102, 103). This technology also provides the ability to directly validate (or refute) the hypotheses generated by PiCnIc via gene correction and single cell perturbation approaches.

To conclude, the precision of any statistical inference technique, including PiCnIc, is influenced by the quality, availability, and idiosyncrasies of the input data—the goodness of the outcomes improving along with the expected advancement in the field. Nevertheless, the strength of the proposed approach lies in

the efficacy in managing possibly noisy/ biased or insufficient data, and in proposing refutable hypotheses for experimental validation.

Materials and Methods

Processing COADREAD Samples with PiCnIc. We instantiated PiCnIc to process clinically annotated high MSI-HIGH and MSS colorectal tumors collected from TCGA project COADREAD (56) (*SI Appendix*, Fig. S1). Details on the implementation and the source code to replicate this study are available in the *SI Appendix*. COADREAD has enough samples, especially for MSS tumors, to implement a consistent and significant statistical validation of our findings (*SI Appendix*, Table S1).

In brief, we split subtypes by the microsatellite status of each tumor as annotated by the consortium (so, step I of PiCnIc is done by exploiting background knowledge rather than computational predictors). It should be expected that if this step is skipped or this classification is incorrect, the resulting models would noticeably differ. Once split into groups, the input COADREAD data are processed to maintain only samples for which both high-quality curated mutation and CNA data are available; for CNAs we use focal high-level amplifications and homozygous deletions.

Then, for each sample we select only alterations (mutations/CNAs) from a list of 33 driver genes manually annotated to five pathways in ref. 56: WNT, RAF, TGF-β, PI3K, and p53 (*SI Appendix*, Figs. S2 and S3). This list of drivers, step II of PiCnIc, is produced by TCGA, as a result of manual curation and running MutSigCV.

In the next module of the pipeline, we fetch groups of exclusive alterations. We scanned these groups by using the MUTEX tool (*SI Appendix*, Table S2) and merged its results with the group that TCGA detected by using the MEMO tool, which involves mainly genes from the PI3K pathway. Knowledge on the potential exclusivity among genes in the WNT (*APC* and *CTNNB1*) and RAF (*KRAS*, *NRAS*, and *BRAF*) pathways was exploited as well. Groups were then used to create CAPRI's formulas; we also included hypotheses for genes that harbor mutations and CNAs across different samples (*SI Appendix*, Table S3). Data and exclusivity groups for MSS tumors are shown in *SI Appendix*, Figs. S4 and S5.

CAPRI was run, as the last step of PiCnIc, on each subtype, by selecting recurrent alterations from the pool of 33 pathway genes and using both AIC/BIC regularizer. Timings to run the relevant steps of the pipeline are reported in the *SI Appendix*. In the models of Figs. 4 and 5 each edge mirrors selective advantage among the upstream and downstream nodes, as estimated by CAPRI; Mann-Withney *U* test is carried out with statistical significance 0.05, after 100 nonparametric bootstrap iterations.

The significance of the reconstructed models and the input data is assessed by computing all of the statistics/tests discussed in the main text (temporal priority, probability raising and hypergeometric testing *P* values, bootstrap, and cross-validation scores). Motivation and background on each of these measures is available in the *SI Appendix*. A table with their values for edges with highest nonparametric bootstrap scores is in *SI Appendix*, Fig. S8.

For the MSS cohort all of the *P* values are strongly significant ($P \ll 0.01$) except for the temporal priority of the edges connecting mutations in *FAM123B* and *ATM*, and *ERBB2* alterations (mutations and amplifications), which leads us to conclude that, even if these pairs of genes seem to undergo selective advantage, the temporal ordering of their occurrence is ambiguous and failed to be imputed correctly from the datasets, analyzed here. The same situation occurs in MSI-HIGH tumors, for the relation between *KRAS* and *ERBB3*. Nonparametric and statistical bootstrap estimations are used to assess the strength of all of the findings (*SI Appendix*, Figs. S6 and S7). Moreover, any bias in the data is finally evaluated by cross-validation (*SI Appendix*, Figs. S8–S11) and common statistics such as entropy loss, posterior classification, and prediction errors. In general, most of the selective advantage relations depicted by the inferred models present a strong statistical support, with the MSS cohort presenting the most reliable results.

Summary implementation for COADREAD (PiCnIc steps; Fig. 2): (*i*) TCGA clinical classification, (*ii*) MutSigCV and TCGA manual curation, (*iii*) MEMO, MUTEX, and knowledge of WNT and RAF pathways, and (*iv*) CAPRI.

Implement Your Own Case Study with PiCnIc/TRONCO. TRONCO started as a project before PiCnIc and is our effort at collecting, in a free R package, algorithms to infer progression models from genomic data. In its current version it offers the implementation of the CAPRI and CAPRESE algorithms, as well as a set of routines to preprocess genomic data. With the introduction of PiCnIc, began to incorporate software routines to easily interface CAPRI and CAPRESE to some of the tools that we mention in Fig. 2. In particular, in its current 2.0 version it supports input/output for the MATLAB Network Based Stratification tool (NBS) and the Java MUTEX tool, as well as the facility to fetch data available from the cBioPortal for Cancer Genomics (www.cbioportal.org), which provides a web resource for exploring, visualizing, and analyzing multidimensional cancer genomics data.

We plan to extend TRONCO in the future to support other similar tools and become an integral part of daily laboratory routines, thus facilitating application of PiCnIc to additional use cases.

ACKNOWLEDGMENTS. We thank the anonymous reviewers and Prof. Giovanni Tonon for their help with improving the quality and rigor of the manuscript. This work was supported by the SysBioNet project, a Ministero dell'Istruzione, dell'Università e della Ricerca initiative for the Italian Roadmap of European Strategy Forum on Research Infrastructures, and Regione Lombardia (Italy) for the research projects RetroNet through ASTIL Program Grant 12-4-5148000-40 (to M.A., G.M., G.C., A.G., and D.R.). This work was also supported by UA 053 and Network Enabled Drug Design Project ID14546A Rif SAL-7, Fondo Accordi Istituzionali 2009, National Science Foundation Grants CCF-0836649 and CCF-0926166, and a National Cancer Institute Physical Sciences-Oncology Center Grant U54 CA193313-01 (to B.M.); and by the Instituto de Salud Carlos III, supported by European Regional Development Fund Grants PI11-01439, PIE13/00022, the Spanish Association Against Cancer Scientific Foundation, and Catalan Government DURSI Grant 2014SGR647 (to V.M. and R.S.-P.).

1. Nowell PC (1976) The clonal evolution of tumor cell populations. *Science* 194(4260):23–28.
2. Fidler IJ (1978) Tumor heterogeneity and the biology of cancer invasion and metastasis. *Cancer Res* 38(9):2651–2660.
3. Dexter DL, et al. (1978) Heterogeneity of tumor cells from a single mouse mammary tumor. *Cancer Res* 38(10):3174–3181.
4. Merlo LM, Pepper JW, Reid BJ, Maley CC (2006) Cancer as an evolutionary and ecological process. *Nat Rev Cancer* 6(12):924–935.
5. Hanahan D, Weinberg RA (2000) The hallmarks of cancer. *Cell* 100(1):57–70.
6. Hanahan D, Weinberg RA (2011) Hallmarks of cancer: The next generation. *Cell* 144(5):646–674.
7. Huang S, Ernberg I, Kauffman S (2009) Cancer attractors: A systems view of tumors from a gene network dynamics and developmental perspective. *Semin Cell Div Biol* 20(7):869–876.
8. Futreal PA, et al. (2004) A census of human cancer genes. *Nat Rev Cancer* 4(3):177–183.
9. Vogelstein B, et al. (2013) Cancer genome landscapes. *Science* 339(6127):1546–1558.
10. Garraway LA, Lander ES (2013) Lessons from the cancer genome. *Cell* 153(1):17–37.
11. Zack TI, et al. (2013) Pan-cancer patterns of somatic copy number alteration. *Nat Genet* 45(10):1134–1140.
12. Baylin SB, Jones PA (2011) A decade of exploring the cancer epigenome - biological and translational implications. *Nat Rev Cancer* 11(10):726–734.
13. Weinberg R (2013) *The Biology of Cancer* (Garland, New York).
14. Albini A, Sporn MB (2007) The tumour microenvironment as a target for chemoprevention. *Nat Rev Cancer* 7(2):139–147.
15. Greaves M, Maley CC (2012) Clonal evolution in cancer. *Nature* 481(7381):306–313.
16. Nowak MA, Michor F, Iwasa Y (2003) The linear process of somatic evolution. *Proc Natl Acad Sci USA* 100(25):14966–14969.
17. Vogelstein B, Kinzler KW (2004) Cancer genes and the pathways they control. *Nat Med* 10(8):789–799.
18. Nowak MA (2006) *Evolutionary Dynamics* (Harvard Univ Press, Cambridge, MA).
19. Wood LD, et al. (2007) The genomic landscapes of human breast and colorectal cancers. *Science* 318(5853):1108–1113.
20. Jones S, et al. (2008) Core signaling pathways in human pancreatic cancers revealed by global genomic analyses. *Science* 321(5897):1801–1806.
21. Parsons DW, et al. (2008) An integrated genomic analysis of human glioblastoma multiforme. *Science* 321(5897):1807–1812.
22. Fisher R, Pusztai L, Swanton C (2013) Cancer heterogeneity: Implications for targeted therapeutics. *Br J Cancer* 108(3):479–485.
23. Curtis C, et al.; METABRIC Group (2012) The genomic and transcriptomic architecture of 2,000 breast tumours reveals novel subgroups. *Nature* 486(7403):346–352.
24. Gerlinger M, et al. (2012) Intratumor heterogeneity and branched evolution revealed by multiregion sequencing. *N Engl J Med* 366(10):883–892.
25. National Cancer Institute; National Genome Research Institute (2015) *The Cancer Genome Atlas* (Natl Inst Health, Bethesda). Available at https://tcga-data.nci.nih.gov/tcga. Accessed March 12, 2015.
26. Navin N, et al. (2011) Tumour evolution inferred by single-cell sequencing. *Nature* 472(7341):90–94.
27. Eberwine J, Sul JY, Bartfai T, Kim J (2014) The promise of single-cell sequencing. *Nat Methods* 11(1):25–27.
28. Beerenwinkel N, Schwarz RF, Gerstung M, Markowetz F (2015) Cancer evolution: Mathematical models and computational inference. *Syst Biol* 64(1):e1–e25.
29. Ramchandani S, Bhattacharya SK, Cervoni N, Szyf M (1999) DNA methylation is a reversible biological signal. *Proc Natl Acad Sci USA* 96(11):6107–6112.

30. Vogelstein B, et al. (1988) Genetic alterations during colorectal-tumor development. *N Engl J Med* 319(9):525–532.
31. Desper R, et al. (1999) Inferring tree models for oncogenesis from comparative genome hybridization data. *J Comput Biol* 6(1):37–51.
32. Desper R, et al. (2000) Distance-based reconstruction of tree models for oncogenesis. *J Comput Biol* 7(6):789–803.
33. Szabo A, Boucher K (2002) Estimating an oncogenetic tree when false negatives and positives are present. *Math Biosci* 176(2):219–236.
34. Beerenwinkel N, et al. (2005) Learning multiple evolutionary pathways from cross-sectional data. *J Comput Biol* 12(6):584–598.
35. Beerenwinkel N, Eriksson N, Sturmfels B (2007) Conjunctive Bayesian networks. *Bernoulli* 13(4):893–909.
36. Gerstung M, Baudis M, Moch H, Beerenwinkel N (2009) Quantifying cancer progression with conjunctive Bayesian networks. *Bioinformatics* 25(21):2809–2815.
37. Attolini CSO, et al. (2010) A mathematical framework to determine the temporal sequence of somatic genetic events in cancer. *Proc Natl Acad Sci USA* 107(41): 17604–17609.
38. Misra N, Szczurek E, Vingron M (2014) Inferring the paths of somatic evolution in cancer. *Bioinformatics* 30(17):2456–2463.
39. Olde Loohuis L, et al. (2014) Inferring tree causal models of cancer progression with probability raising. *PLoS One* 9(10):e108358.
40. Ramazzotti D, et al. (2015) CAPRI: Efficient inference of cancer progression models from cross-sectional data. *Bioinformatics* 31(18):3016–3026.
41. De Sano L, et al. (2016) TRONCO: An R package for the inference of cancer progression models from heterogeneous genomic data. *Bioinformatics*, 10.1093/bioinformatics/btw035.
42. Suppes P (1970) *A Probabilistic Theory of Causality* (North-Holland, Amsterdam).
43. Navin NE (2014) Cancer genomics: One cell at a time. *Genome Biol* 15(8):452.
44. Wang Y, et al. (2014) Clonal evolution in breast cancer revealed by single nucleus genome sequencing. *Nature* 512(7513):155–160.
45. Gerlinger M, et al. (2014) Genomic architecture and evolution of clear cell renal cell carcinomas defined by multiregion sequencing. *Nat Genet* 46(3):225–233.
46. Oesper L, Mahmoody A, Raphael BJ (2013) THetA: Inferring intra-tumor heterogeneity from high-throughput DNA sequencing data. *Genome Biol* 14(7):R80.
47. Oesper L, Satas G, Raphael BJ (2014) Quantifying tumor heterogeneity in whole-genome and whole-exome sequencing data. *Bioinformatics* 30(24):3532–3540.
48. Miller CA, et al. (2014) SciClone: Inferring clonal architecture and tracking the spatial and temporal patterns of tumor evolution. *PLOS Comput Biol* 10(8):e1003665.
49. Roth A, et al. (2014) PyClone: Statistical inference of clonal population structure in cancer. *Nat Methods* 11(4):396–398.
50. Jiao W, Vembu S, Deshwar AG, Stein L, Morris Q (2014) Inferring clonal evolution of tumors from single nucleotide somatic mutations. *BMC Bioinformatics* 15:35.
51. Fischer A, Vázquez-García I, Illingworth CJ, Mustonen V (2014) High-definition reconstruction of clonal composition in cancer. *Cell Reports* 7(5):1740–1752.
52. Zare H, et al. (2014) Inferring clonal composition from multiple sections of a breast cancer. *PLOS Comput Biol* 10(7):e1003703.
53. Garvin T, et al. (2015) Interactive analysis and assessment of single-cell copy-number variations. *Nat Methods* 12(11):1058–1060.
54. Malikic S, McPherson AW, Donmez N, Sahinalp CS (2015) Clonality inference in multiple tumor samples using phylogeny. *Bioinformatics* 31(9):1349–1356.
55. El-Kebir M, Oesper L, Acheson-Field H, Raphael BJ (2015) Reconstruction of clonal trees and tumor composition from multi-sample sequencing data. *Bioinformatics* 31(12):i62–i70.
56. Cancer Genome Atlas Network (2012) Comprehensive molecular characterization of human colon and rectal cancer. *Nature* 487(7407):330–337.
57. Ley TJ, et al.; Cancer Genome Atlas Research Network (2013) Genomic and epigenomic landscapes of adult de novo acute myeloid leukemia. *N Engl J Med* 368(22): 2059–2074.
58. Creighton CJ, et al.; Cancer Genome Atlas Research Network (2013) Comprehensive molecular characterization of clear cell renal cell carcinoma. *Nature* 499(7456):43–49.
59. Bennett JM, et al. (1976) Proposals for the classification of the acute leukaemias. French-American-British (FAB) co-operative group. *Br J Haematol* 33(4):451–458.
60. Lu J, et al. (2005) MicroRNA expression profiles classify human cancers. *Nature* 435(7043):834–838.
61. Gao Y, Church G (2005) Improving molecular cancer class discovery through sparse non-negative matrix factorization. *Bioinformatics* 21(21):3970–3975.
62. de Souto MC, Costa IG, de Araujo DS, Ludermir TB, Schliep A (2008) Clustering cancer gene expression data: A comparative study. *BMC Bioinformatics* 9:497.
63. Bell D, et al.; Cancer Genome Atlas Research Network (2011) Integrated genomic analyses of ovarian carcinoma. *Nature* 474(7353):609–615.
64. Konstantinopoulos PA, et al. (2010) Gene expression profile of BRCAness that correlates with responsiveness to chemotherapy and with outcome in patients with epithelial ovarian cancer. *J Clin Oncol* 28(22):3555–3561.
65. Reis-Filho JS, Pusztai L (2011) Gene expression profiling in breast cancer: Classification, prognostication, and prediction. *Lancet* 378(9805):1812–1823.
66. Hofree M, Shen JP, Carter H, Gross A, Ideker T (2013) Network-based stratification of tumor mutations. *Nat Methods* 10(11):1108–1115.
67. Zhong X, Yang H, Zhao S, Shyr Y, Li B (2015) Network-based stratification analysis of 13 major cancer types using mutations in panels of cancer genes. *BMC Genomics* 16:(Suppl 7):S7.
68. Lawrence MS, et al. (2013) Mutational heterogeneity in cancer and the search for new cancer-associated genes. *Nature* 499(7457):214–218.
69. Gonzalez-Perez A, Lopez-Bigas N (2012) Functional impact bias reveals cancer drivers. *Nucleic Acids Res* 40(21):e169.
70. Tamborero D, Gonzalez-Perez A, Lopez-Bigas N (2013) OncodriveCLUST: Exploiting the positional clustering of somatic mutations to identify cancer genes. *Bioinformatics* 29(18):2238–2244.
71. Dees ND, et al. (2012) MuSiC: Identifying mutational significance in cancer genomes. *Genome Res* 22(8):1589–1598.
72. Tamborero D, Lopez-Bigas N, Gonzalez-Perez A (2013) Oncodrive-CIS: A method to reveal likely driver genes based on the impact of their copy number changes on expression. *PLoS One* 8(2):e55489.
73. Gundem G, et al. (2010) IntOGen: Integration and data mining of multidimensional oncogenomic data. *Nat Methods* 7(2):92–93.
74. Yeang CH, McCormick F, Levine A (2008) Combinatorial patterns of somatic gene mutations in cancer. *FASEB J* 22(8):2605–2622.
75. Miller CA, Settle SH, Sulman EP, Aldape KD, Milosavljevic A (2011) Discovering functional modules by identifying recurrent and mutually exclusive mutational patterns in tumors. *BMC Med Genomics* 4:34.
76. Ciriello G, Cerami E, Sander C, Schultz N (2012) Mutual exclusivity analysis identifies oncogenic network modules. *Genome Res* 22(2):398–406.
77. Babur Ö, et al. (2015) Systematic identification of cancer driving signaling pathways based on mutual exclusivity of genomic alterations. *Genome Biol* 16:45.
78. Vandin F, Upfal E, Raphael BJ (2012) De novo discovery of mutated driver pathways in cancer. *Genome Res* 22(2):375–385.
79. Zhao J, Zhang S, Wu LY, Zhang XS (2012) Efficient methods for identifying mutated driver pathways in cancer. *Bioinformatics* 28(22):2940–2947.
80. Leiserson MD, Blokh D, Sharan R, Raphael BJ (2013) Simultaneous identification of multiple driver pathways in cancer. *PLOS Comput Biol* 9(5):e1003054.
81. Leiserson MDM, Wu HT, Vandin F, Raphael BJ (2015) CoMEt: A statistical approach to identify combinations of mutually exclusive alterations in cancer. *Genome Biol* 16:160.
82. Hua X, et al. (2016) MEGSA: A powerful and flexible framework for analyzing mutual exclusivity of tumor mutations. *Am J Hum Genet* 98(3):442–455.
83. Szczurek E, Beerenwinkel N (2014) Modeling mutual exclusivity of cancer mutations. *PLOS Comput Biol* 10(3):e1003503.
84. Leiserson MD, et al. (2015) Pan-cancer network analysis identifies combinations of rare somatic mutations across pathways and protein complexes. *Nat Genet* 47(2):106–114.
85. Vandin F, Upfal E, Raphael BJ (2011) Algorithms for detecting significantly mutated pathways in cancer. *J Comput Biol* 18(3):507–522.
86. Efron B, Tibshirani RJ (1994) *An Introduction to the Bootstrap* (CRC, Boca Raton, FL).
87. Koller D, Friedman N (2009) *Probabilistic Graphical Models: Principles and Techniques*. Adaptive Computation and Machine Learning Series (MIT Press, Cambridge, MA).
88. Ogino S, Goel A (2008) Molecular classification and correlates in colorectal cancer. *J Mol Diagn* 10(1):13–27.
89. Fearon ER, Vogelstein B (1990) A genetic model for colorectal tumorigenesis. *Cell* 61(5):759–767.
90. Vilar E, Gruber SB (2010) Microsatellite instability in colorectal cancer-the stable evidence. *Nat Rev Clin Oncol* 7(3):153–162.
91. Abdel-Samad R, et al. (2011) MiniSOX9, a dominant-negative variant in colon cancer cells. *Oncogene* 30(22):2493–2503.
92. Kormish JD, Sinner D, Zorn AM (2010) Interactions between SOX factors and Wnt/β-catenin signaling in development and disease. *Dev Dyn* 239(1):56–68.
93. Li L, et al. (2014) Sequential expression of miR-182 and miR-503 cooperatively targets FBXW7, contributing to the malignant transformation of colon adenoma to adenocarcinoma. *J Pathol* 234(4):488–501.
94. Kim JH, Kang GH (2014) Molecular and prognostic heterogeneity of microsatellite-unstable colorectal cancer. *World J Gastroenterol* 20(15):4230–4243.
95. Deming DA, et al. (2014) PIK3CA and APC mutations are synergistic in the development of intestinal cancers. *Oncogene* 33(17):2245–2254.
96. Kim MS, Kim SS, Ahn CH, Yoo NJ, Lee SH (2009) Frameshift mutations of Wnt pathway genes AXIN2 and TCF7L2 in gastric carcinomas with high microsatellite instability. *Hum Pathol* 40(1):58–64.
97. Muto Y, et al. (2014) DNA methylation alterations of AXIN2 in serrated adenomas and colon carcinomas with microsatellite instability. *BMC Cancer* 14:466.
98. Zhan P, et al. (2015) FBXW7 negatively regulates ENO1 expression and function in colorectal cancer. *Lab Invest* 95(9):995–1004.
99. Guinney J, et al. (2015) The consensus molecular subtypes of colorectal cancer. *Nat Med* 21(11):1350–1356.
100. Loohuis LO, Witzel A, Mishra B (2014) Cancer hybrid automata: Model, beliefs and therapy. *Inf Comput* 236:68–86.
101. Korsunsky I (2016) Survival analysis using probabilistic graphical models and probabilistic causation with applications to cancer genomics. PhD thesis (New York University, New York).
102. Reed J, et al. (2012) Identifying individual DNA species in a complex mixture by precisely measuring the spacing between nicking restriction enzymes with atomic force microscope. *J R Soc Interface* 9(74):2341–2350.
103. Sundstrom A, et al. (2012) Image analysis and length estimation of biomolecules using AFM. *IEEE Trans Inf Technol Biomed* 16(6):1200–1207.